Ceramics International 48 (2022) 3199–3205

Contents lists available at ScienceDirect

Ceramics International

journal homepage: www.elsevier.com/locate/ceramint

Highly sensitive characteristic of surface enhanced Raman scattering for CuO/Au core/shell nanowires substrate

Thi Ha Tran [a,b,**], Thi Mai Anh Nguyen [c], Vu Phuong Thao Dao [b], Cong Doanh Sai [b], Thanh Cong Bach [b], Nguyen Hai Pham [b,***], An Bang Ngac [b], Van Thanh Pham [b], Thi Kim Chi Tran [d], Hyeonsik Cheong [e], Viet Tuyen Nguyen [b,*]

[a] Hanoi University of Mining and Geology, 18 Vien Street, Duc Thang, Bac Tu Liem, Hanoi, Viet Nam
[b] Faculty of Physics, University of Science, Vietnam National University, Hanoi, 334 Nguyen Trai, Thanh Xuan, Hanoi, Viet Nam
[c] HUS High School for Gifted Students, 182 Luong the Vinh, Thanh Xuan, Hanoi, Viet Nam
[d] Institute of Materials Science, Vietnam Academy of Science and Technology, 18 Hoang Quoc Viet, Cau Giay, Hanoi, Viet Nam
[e] Department of Physics, Sogang University, Seoul, 04107, South Korea

ARTICLE INFO

Keywords:
CuO nanowires
Thermal oxidation
Sputtering
Surface enhanced Raman scattering

ABSTRACT

In this paper, we report a facile process to fabricate CuO/Au core/shell nanowires, where CuO core and Au shell were prepared by thermal oxidation and sputtering, respectively. The as-prepared CuO/Au nanowires are highly sensitive surface-enhanced-Raman-scattering (SERS) substrates, which can detect methylene blue down to a very low concentration of 10^{-13} M. The major advantages of SERS substrates based on CuO/Au core/shell nanowires compared with others SERS substrates are the high sensitivity, uniformity, and purity due to the absence of any organic surfactants in the synthesis process.

1. Introduction

Optical spectroscopic methods are interesting since they are usually sensitive, molecule-specific in some cases, and low cost. Among available optical methods, Raman scattering might be the most promising solution because it offers fingerprints of molecules through their own unique sets of vibrational modes [1–3]. Raman scattering is well-known for its applications in material science [4–6] thanks to many advantages such as: time-saving, convenient, and nondestructive technique, offering characteristic spectra, etc. The discovery of the surface enhanced Raman scattering (SERS) technique has extended its application to other fields such as: biomedical or environmental analysis where detection of substance at trace level is normally an inevitable requirement [7,8]. For decades, a major topic in SERS research is to develop noble metal SERS substrates of high enhancement and good reproducibility [9–11]. Such features can be attained by electron beam lithography technique but the substrates prepared by this method are available only at laboratory scale due to their high cost and small active area [12]. A more practical approach is utilization of chemical processes, which can produce affordable SERS substrate of large area at the cost of enhancement and uniformity. Furthermore, the usage of surfactants in the synthesis process can lead to unavoidable residues in the obtained SERS substrates.

Recently, some hybrid structures of ordered semiconductor nanostructures and noble metals were developed as potential SERS substrates, which can take advantages of both semiconductor and noble metal properties to achieve better repeatability and Raman sensitivity at a reasonable cost. A number of composites of semiconductor nanostructures and noble metals have been studied such as: TiO_2 [13–15], ZnO [16–20], Si [21], SiO_2–Si [22], SiO_2-WO_3 [23], Al_2O_3 [24] etc. CuO is a well-known p type semiconductor with many interesting properties such as: a small band gap, strong field emission, photocatalytic properties, etc. However, in the field of SERS, CuO is less studied than other oxide semiconductors. Also, among available studies on composites of semiconductors and noble metals for SERS application in the literature, CuO nanostructures were mostly prepared by chemical approaches and most studies focused on CuO nanoparticles only. In fact, there are still some short comings from these structures such as: complexity in synthesis, or using toxic and/or organic precursors which might lead to

* Corresponding author.
** Corresponding author. Hanoi University of Mining and Geology, 18 Vien Street, Duc Thang, Bac Tu Liem, Hanoi.
*** Corresponding author.
E-mail addresses: tranthiha@humg.edu.vn (T.H. Tran), phamnguyenhai@hus.edu.vn (N.H. Pham), nguyenviettuyen@hus.edu.vn (V.T. Nguyen).

https://doi.org/10.1016/j.ceramint.2021.10.093
Received 8 July 2021; Received in revised form 16 October 2021; Accepted 18 October 2021
Available online 19 October 2021

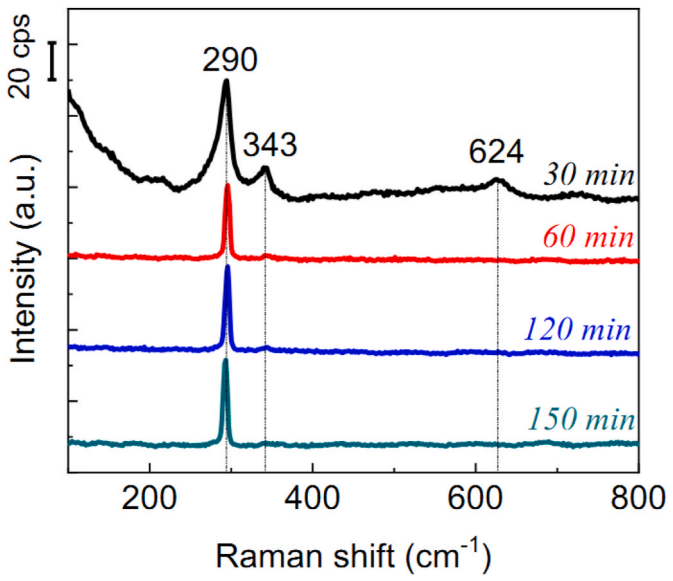

Fig. 1. Raman spectra of CuO nanowires prepared by thermal oxidation at 500 °C in different annealing time.

interference with the signal of the Raman probe.

It has been known that thermal oxidation is one of few physical methods that can be used to synthesize metal oxide nanostructures with many benefits such as: low cost, simplicity, high throughput yield, purity, no requirement of surface treatment with surfactant, and a large scale synthesis. In our previous work [25], we reported CuO/Ag nanowires as effective SERS substrates which could detect methylene blue (MB) at a low concentration of 10^{-11} M. However, due to oxidation process, Ag is less substantial than Au and limits the stability of the prepared SERS substrate. In this paper, we propose to use CuO/Au core/shell nanowires as an active and stable SERS substrate. CuO nanowires were prepared by the thermal oxidation method and gold nano shells were then coated onto CuO nanowires by sputtering. The process is facile and environment friendly without using any organic precursors, and thus offers SERS substrates of highest purity with excellent enhancement capability and repeatability. The chemical and physical stability of CuO and Au guarantees the steady state of the as-prepared SERS substrates.

2. Experiment

CuO nanowires were prepared by thermal oxidation. Details of the synthetic process were described elsewhere [26]. In a typical process, copper substrates in form of copper wires (1 mm in diameter and 3 cm in length) were cleaned with diluted HCl 10% in 1 h before being washed thoroughly with double distilled water, ethanol and acetone in sequence in 5 cycles (10 min each cycle) by ultrasonic bath. The substrates were then transferred into a horizontal furnace for thermal oxidation in open air at 500 °C in different annealing time: 30, 60, 120 and 150 min. The heating rate was 5 °C/min. The obtained products are quite well aligned CuO nanowires of uniform sizes. Gold was then sputtered on the as-prepared CuO nanowires to obtain core/shell nanowires by using JFC-1200 DC sputtering system. The sputtering current was kept at 20

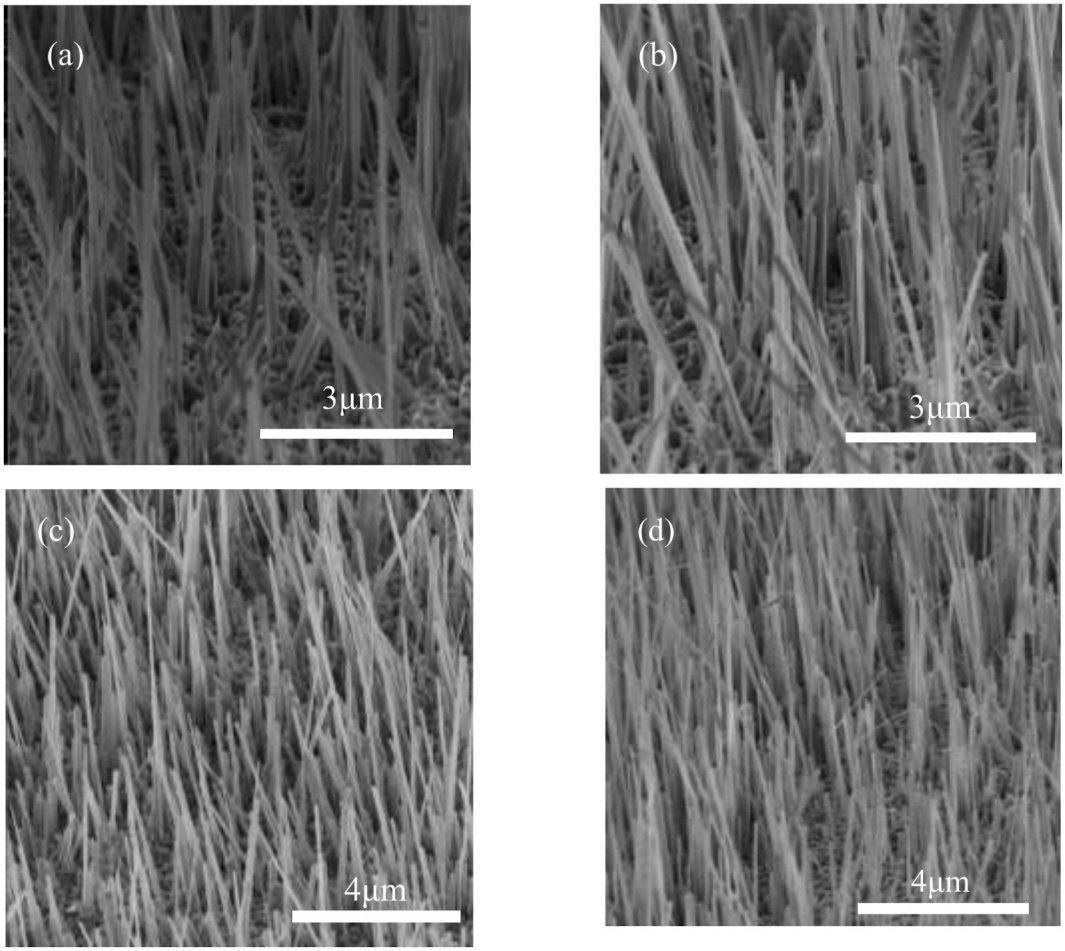

Fig. 2. SEM images of CuO nanowires annealed at 500 °C in: a) 30 min, b) 60 min, c) 120 min, d) 150 min.

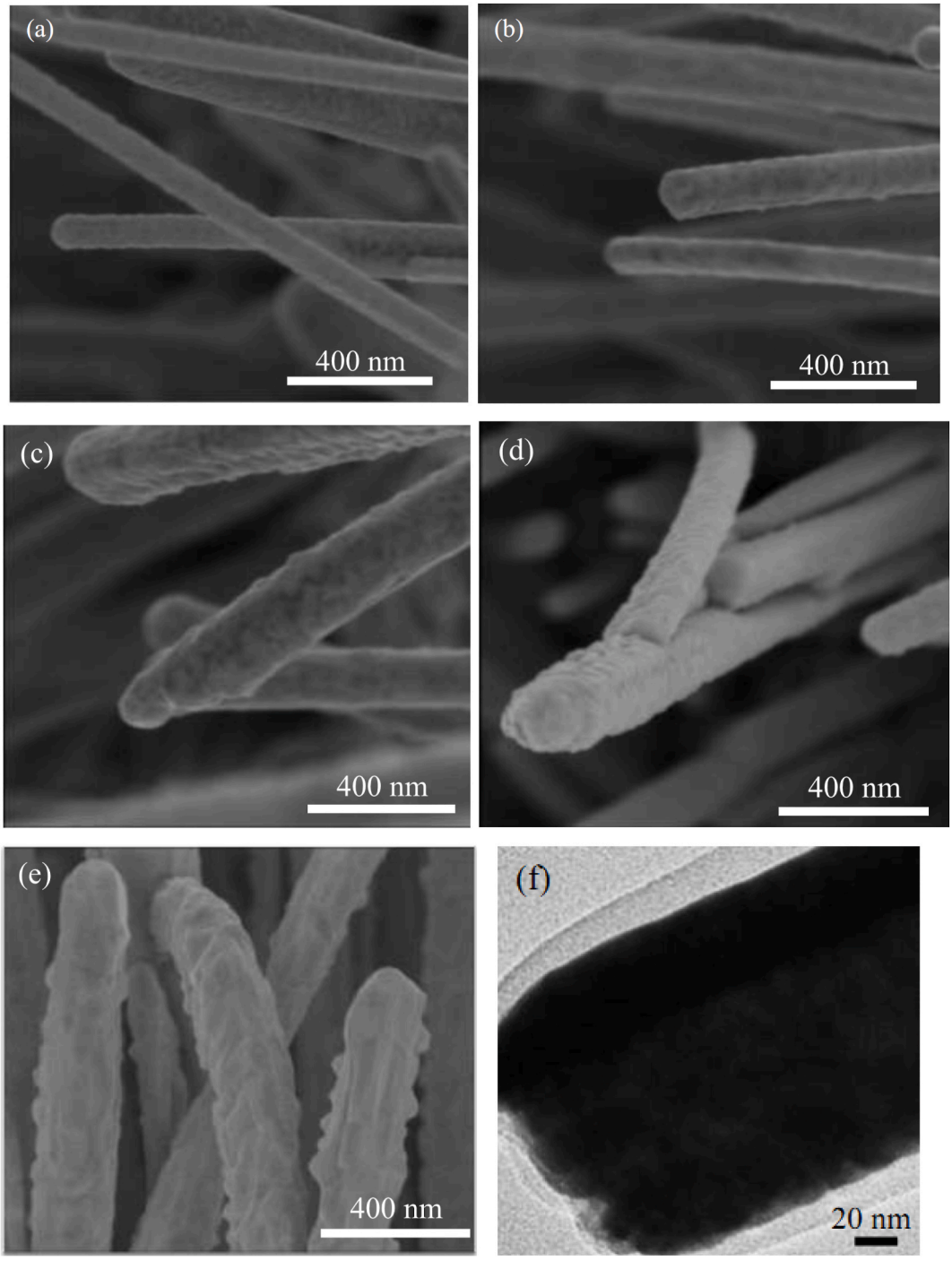

Fig. 3. SEM image of CuO nanowires prepared at 500 °C in 120 min coated with Au of different thickness: a) 20 nm; b) 40 nm; c) 80 nm; d) 160 nm and e) 240 nm and f) HRTEM image of a CuO/Au core/shell nanowire.

mA and the shell thickness can be conveniently controlled by varying the sputtering time. The base pressure during the sputtering process was maintained at about 6 Pa. To investigate the effect of the gold shell layer on the Raman enhancement capacity, a set of samples was prepared with the estimated shell layer of 20, 40, 80, 160 and 240 nm. For SERS investigation, equal volumes of MB solutions (20 μL) of different concentrations were directly dropped onto CuO/Au core/shell nanowire samples. After being dried naturally, the samples were ready for SERS measurements.

The morphology and size of the nanostructures were investigated by a scanning electron microscope (Nova Nano SEM Fei 450). The elemental composition of the samples was studied by using an energy dispersive spectroscopy (EDS) integrated in the SEM system. The Raman spectra of the samples were collected on a confocal Labram HR 800 Raman system (Horiba Jobin Yvon). The samples were excited with the 632.8-nm line of a He–Ne laser, with a power of 0.25 mW at the surface of the samples. A 50X long working distance objective len, which offered a laser spot of about 2 μm diameter, was used to collect Raman signal. The integration time for SERS measurement varied from 30 s to 90 s.

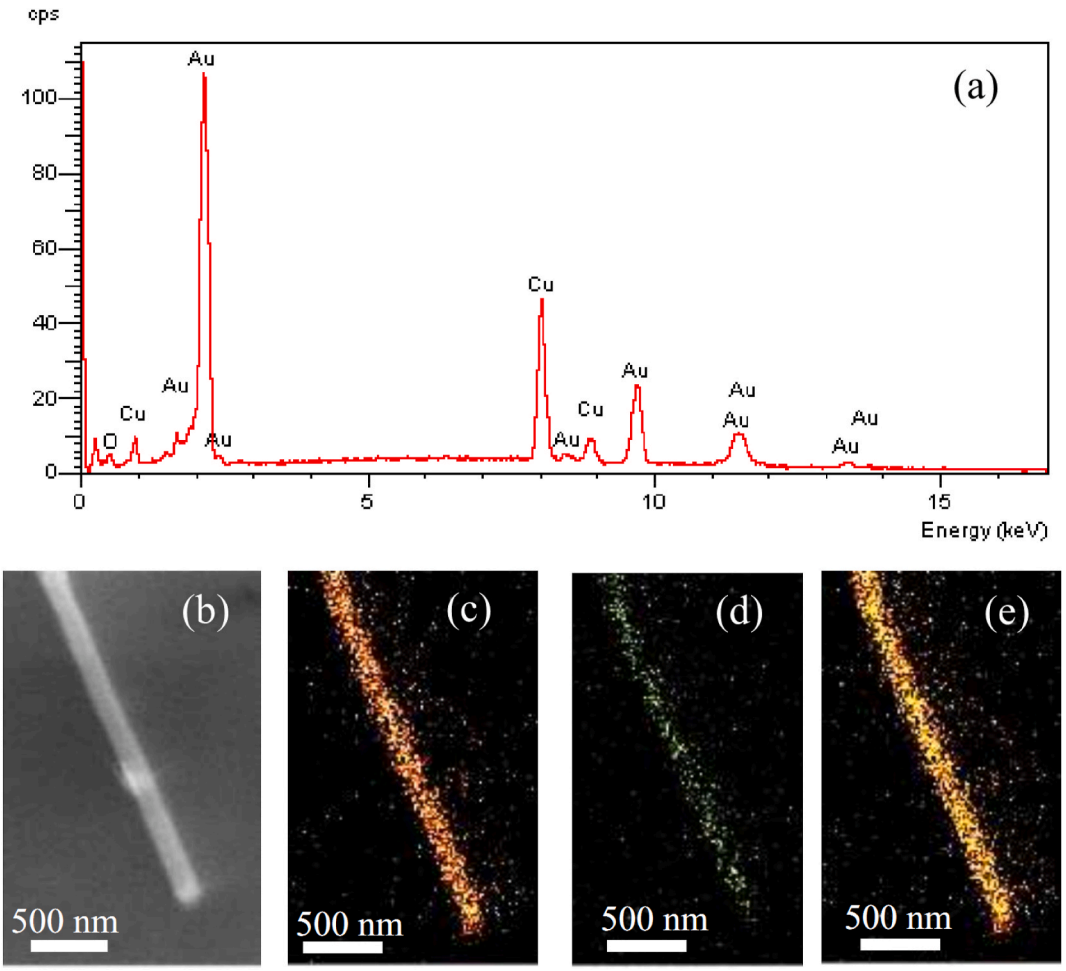

Fig. 4. EDS spectrum of CuO/Au nanowires prepared with shell thickness of 20 nm (a); Compositional elemental mapping of a CuO/Au core-shell nanowire prepared with shell thickness of 20 nm: (b) Scanning electron microscopy image of a core-shell nanowire, elemental maps of (c) Au, (d) Cu elements and (e) overlay mapping of Cu and Au elements.

3. Results and discussion

CuO has three Raman active modes: A_g at around 290 cm^{-1}, and two B_g modes at ~ 343 cm^{-1} and 624 cm^{-1} [27]. It can be seen from Fig. 1 that at all annealing time, the main product is CuO demonstrated by a strong characteristic Raman peak at 290 cm^{-1} and a weaker peak at 343 cm^{-1}. However, the weak Raman peak at around 200 cm^{-1} in the Raman spectrum of sample annealed in 30 min shows a trace of Cu_2O, which is formed right above the Cu substrate at the first stage of the growth [26].

As the annealing time is increased, the characteristic Raman peaks of Cu_2O disappear. This fact can be explained that the growth of longer CuO nanowires at higher density prevents laser from reaching the Cu_2O layer underneath. At the same time, the peak at 292 cm^{-1} becomes narrower and the relative intensity between A^1_g and B^1_g peak of CuO

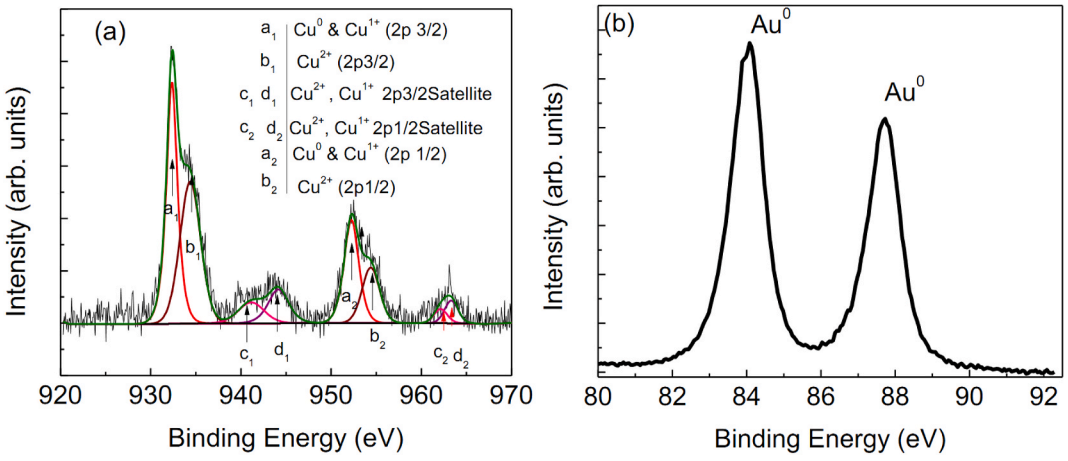

Fig. 5. XPS spectrum of CuO/Au nanowires: (a) Cu_{2p} spectrum and (b) Au_{4f} spectrum.

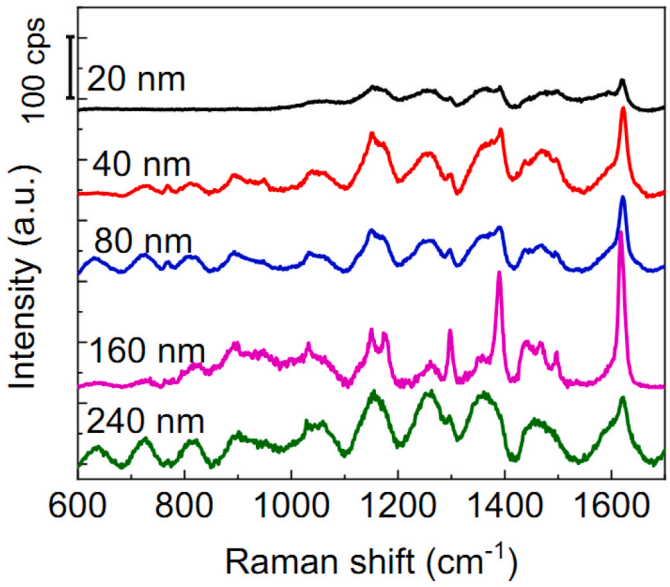

Fig. 6. Raman spectra of 10^{-9} M MB measure on CuO/Au core/shell nanowires of different shell thicknesses.

gets higher. These results likely suggest that the aspect ratio of CuO nanowires becomes larger at longer annealing time [26,28] or in other words, prolonging the annealing time will result in the formation of longer nanowires.

The SEM images of CuO nanowires prepared with different annealing times are shown in Fig. 2. When the annealing time was 30 min or 60 min, some empty areas without nanowires can be observed. When the annealing time is increased to 120 min, the nanowires are grown at high density while the preferred orientation perpendicular to the substrate is still maintained well. When the annealing time is further increased to 150 min, longer nanowires were obtained but a number of nanowires became slightly bended, which degrades the alignment of nanowires. The results suggested that the annealing time of 120 min offers products of the highest quality with high density, uniform size and morphology, and good preferred orientation.

The as-prepared CuO nanowires with 120-min annealing were then sputtered with gold to form core/shell structures. Fig. 3 shows the SEM images of the CuO nanowires annealed at 500 °C for 120 min coated with Au of different thickness. The preferred orientation of the nanowires is maintained after the sputtering process. HRTEM image of a CuO/Au core/shell nanowire (Fig. 3f) clearly shows the core/shell structure of the nanoproduct.

The composition of CuO/Au nanowires was further studied by EDS as shown in Fig. 4a. The EDS results show that the obtained CuO nanowires are composed of only Cu and O elements since CuO/Au nanowires contain Cu, O and Au only. Fig. 4b–e shows elemental mapping by energy dispersive spectroscopy combined with scanning electron microscopy of a CuO/Au nanowire. The results show that Au appears to be distributed over the surface and Cu is mostly in the core. The overlay image also reveals the presence of Au in the shell of the nanowire.

Fig. 5a shows the XPS spectra of CuO/Au nanowires. The deconvolution results show that the Cu_{2p} signal is dominated by species in the Cu^{2+} state with the presence of a small contribution of reduced species Cu^{+} and non-oxidized Cu. While the signal of Cu^{+} results from the Cu_2O layer formed at the initial stage of the growth as discussed in our previous study [26], the Cu signal comes from the substrate. The oxidation state of the Au species in the prepared CuO/Au nanowires was also studied by the XPS test (Fig. 5b). Two characteristic peaks of gold were observed: the Au $4f_{7/2}$ peak at 84.0 eV and the Au $4f_{5/2}$ peak centered at 87.8 eV. No other peak could be deconvoluted. The peak positions match well with the standard values of bulk Au metal. The XPS results suggest that the sputtering process transfers effectively Au from the gold target onto the nanoshell in CuO/Au nanowires while maintaining its metallic state. The metallic state is important to the SERS activity of CuO/Au nanowires.

To demonstrate the SERS activity of the CuO/Au nanowire samples, MB was used as a standard analyte. The sample with a shell thickness of 160 nm was selected for detailed investigation because of its highest enhancement for the same analyte concentration as shown in Fig. 6. Recently, different hetero-nanostructures were developed as a novel type SERS substrate thanks to their advantages over metal nanostructures. In most papers, the authors reported of enhancement of SERS signal of nanocomposites of semiconductor and noble metal nanomaterials compared to individual components. The enhancement is partially resulted from the separation of electron - hole pairs at the interface of heteronanostructures as well as the charge transfer between analytes and SERS substrates as discussed in details by Zhou et al. for Molybdenum Oxide/Tungsten Oxide nano-heterojunction [29], Ag/Ag doped TiO_2 [13] and Hsieh et al. for Ag/CuO nanocomposite [30]. In our case, we also believed that charge transfer between CuO core and gold shell also plays a part on the total Raman enhancement. Such charge transfer transition may induce a strong local electromagnetic field at interface and results in effective Raman enhancement. However, if the shell is too thick, the effect of such electromagnetic field at the interface should fade out because the analyte locates far from this enhanced field.

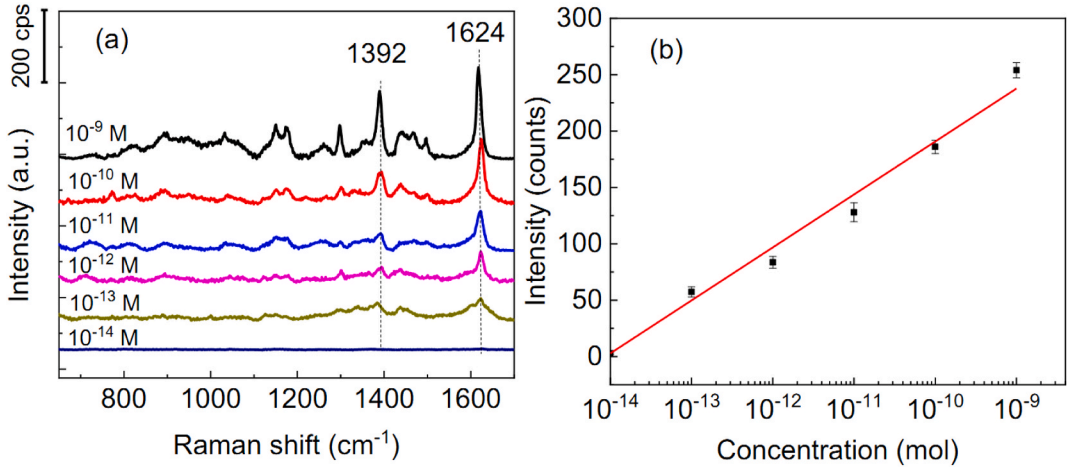

Fig. 7. a) Raman spectra of MB of different concentration dropped on CuO/Au nanowires, and b) A calibration curve where the peak intensity measured at 1624 $cm^{-1}$is plotted versus the logarithmic concentration of MB. Error bars were calculated from 10 different measurements.

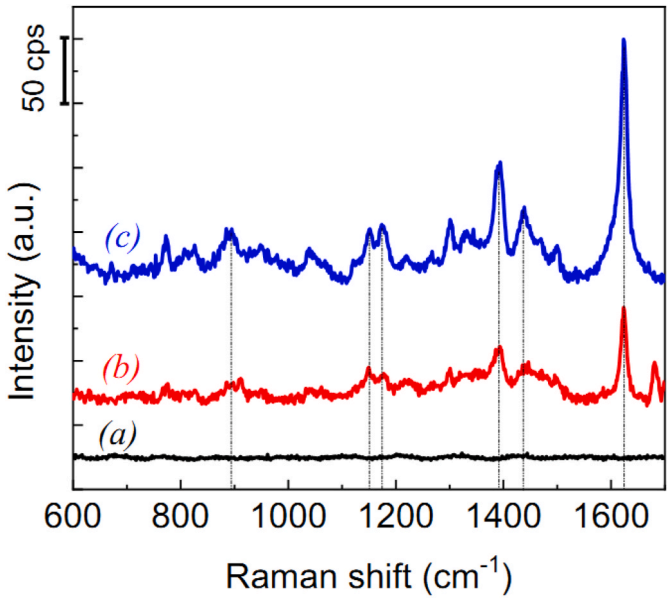

Fig. 8. Raman spectra of a) 10^{-10} M MB dropped on CuO nanowires, b) 10^{-3} M MB on bare CuO nanowires, c) 10^{-10} M MB on CuO/Au nanowires.

This explains for the existence of an optimum thickness as observed.

Fig. 7a shows the Raman spectra of MB with concentrations ranging from 10^{-14} M to 10^{-9} M dropped on CuO/Au nanowires (Raman spectra of MB with concentrations ranging from 10^{-8} M to 10^{-5} M dropped on CuO/Au nanowires are shown in Fig. S1, Supporting Information). As shown in Fig. 7a, even at the ultralow concentration (10^{-13} M), characteristic peaks of MB can be still observed clearly at 1624 and 1392 cm^{-1}. The result shows that CuO/Au nanowires substrate can serve as SERS substrate with a high sensitivity. The dependence of SERS intensity on MB concentration was investigated. The variation of Raman intensity of the peak at 1624 cm^{-1} shows a linear dependence on the MB concentration in the measured range with an excellent correlation coefficient of $R^2 = 0.98$ as shown in Fig. 7 b. The results demonstrate the good correlation between SERS intensity and concentration of MB.

The fitting curve of the experimental data was achieved as: $y = 47.0x + 661$. The limit of detection (LOD), which is the concentration at which the signal to noise ratio equals 3 [31,32], is 7.10^{-14} M.

The enhancement factor (EF) is usually used to evaluate the SERS substrate performance. The experimental value of EF is defined as:

$$EF = \frac{I_{SERS}}{I_{Normal}} . \frac{N_{Normal}}{N_{SERS}},$$

where, I_{SERS} and I_{Normal} are normalized Raman intensities collected with and without using the SERS substrate, N_{Normal} and N_{SERS} are number of probe molecules excited in the excitation volume by the laser. In our case, for reference, MB was dropped on an uncoated CuO nanowires sample prepared at the same condition. Due to its similar morphology of CuO/Au nanowire SERS sample and the bare CuO nanowires as reference sample, it is convenient to replace the number of probe molecules by the corresponding concentration of MB. In all Raman measurements, same volumes of analytes were used and so the EF can be then calculated by:

$$EF = \frac{I_{SERS}}{I_{Normal}} . \frac{C_{Normal}}{C_{SERS}},$$

where, C_{Normal} is the concentration of MB solution dropped on CuO nanowires sample (10^{-3} M), C_{SERS} is the concentration of MB solution dropped on SERS substrate (10^{-10} M).

It should be noted that the concentration of MB (10^{-3} M) is much higher in the reference sample due to the limitation in Raman intensity without enhancement. As shown in Fig. 8, no Raman signal was collected when MB 10^{-10} M is dropped on bared CuO nanowires due to a small Raman scattering cross-section of MB. Clear Raman peaks of MB was observed when measured on CuO/Au nanowires. The experimental EF estimated for the strongest peak at 1624 cm^{-1} was 2×10^7 for the 10^{-10} M solution. Such high enhancement factor is extremely important for detection of substances at low concentration.

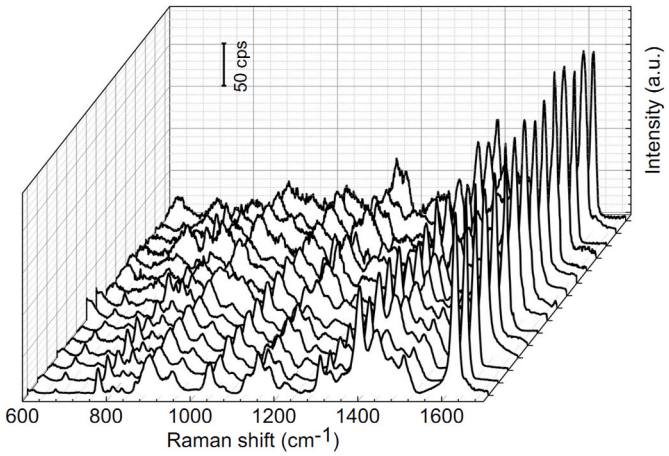

Fig. 9. SERS spectra of 10^{-10} M MB measured at 15 different points on CuO/Au nanowires substrate.

The uniformity of the SERS substrate is a key parameter for reliable SERS detection. Raman spectra of 10^{-10} M MB measured at 15 different random points on CuO/Au nanowire based SERS substrate was presented in Fig. 9. The characteristic peaks of MB appear in all spectra. The small relative standard deviation (RSD) of 8.3% and 11.52% were obtained for the notable peaks at 1624 and 1392 cm^{-1}. These values are comparable with the RSDs of high quality SERS substrates reported by other groups [31,32]. The small RSDs imply that CuO/Au nanowires can be used as reliable SERS substrates of high uniformity.

The excellent Raman enhancement capability of our CuO/Au-nanowires-based SERS substrates is attributed to the combination of several factors. First, the distribution of nanoshell in 3D is expected to provide more hotspots for SERS enhancement [10] compared with a conventional SERS substrate, where noble metal nanoparticles are distributed on a flat 2D surface. Second, the charge transition occurring at the interface of CuO semiconductor and Au metal can create an area of electromagnetic enhancement for boosting the Raman signal. The work function of Au is ~5.1 eV [33], close to the Fermi level of CuO (~5.3 eV) [34]. Therefore, electrons will transfer from Au to CuO until the two Fermi levels are aligned and an equilibrium is achieved. Such charge redistribution will form a junction at the interface with positive charge on the Au side and negative charge on CuO side. The induced electric field in turn will result in tremendous SERS intensity. The charge-transfer-induced polarization mechanism for SERS was also observed in several semiconductor/noble metal systems such as: ZnO/Au [17], ZnO/Ag [35], Cu_2O/Ag, Cu_2O/Au [36].

4. Conclusion

We demonstrated a facile method combining thermal oxidation and sputtering to fabricate active SERS substrates based on CuO/Au core/shell nanowires of controllable shell thickness, high uniformity and preferred orientation. The as-prepared CuO/Au nanowires can serve as high sensitivity SERS substrates. At the optimum thickness of Au shell of 160 nm, CuO/Au nanowires allow to detect MB at a very low concentration of 10^{-13} M. Our approach provides a promising, reliable tool for detecting substances at trace level for applications in biomedical or environmental field.

Declaration of competing interest

The authors declare that they have no known competing financial interests or personal relationships that could have appeared to influence the work reported in this paper.

Acknowledgement

The research was financially supported by VNU Asia Research Center and Chey Institute for Advanced Studies (Project CA.19.6A). Ms. Thi Ha Tran was funded by Vingroup Joint Stock Company and supported by the Domestic Master/PhD Scholarship Programme of Vingroup Innovation Foundation (VINIF), Vingroup Big Data Institute (VINBIGDATA).

Appendix A. Supplementary data

Supplementary data to this article can be found online at https://doi.org/10.1016/j.ceramint.2021.10.093.

References

[1] L. Martín-Carrón, A. De Andrés, M.J. Martínez-Lope, M.T. Casais, J.A. Alonso, Raman phonons as a probe of disorder, fluctuations, and local structure in doped and undoped orthorhombic and rhombohedral manganites, Phys. Rev. B Condens. Matter 66 (2002) 1–8, https://doi.org/10.1103/PhysRevB.66.174303.

[2] V.T. Nguyen, D. Nam, M. Gansukh, S.N. Park, S.J. Sung, D.H. Kim, J.K. Kang, C. D. Sai, T.H. Tran, H. Cheong, Influence of sulfate residue on Cu 2 ZnSnS 4 thin films prepared by direct solution method, Sol. Energy Mater. Sol. Cells 136 (2015) 113–119, https://doi.org/10.1016/j.solmat.2015.01.003.

[3] T.H. Tran, T.H. Pham, C.D. Sai, T.T. Nguyen, V.T. Nguyen, Study phase evolution of hydrothermally synthesized Cu 2 ZnSnS 4 nanocrystals by Raman spectroscopy, Nano-Structures and Nano-Objects 18 (2019), 100273, https://doi.org/10.1016/j.nanoso.2019.100273.

[4] T.H. Tran, T.H. Phi, H.N. Nguyen, N.H. Pham, C.V. Nguyen, K.H. Ho, Q.K. Doan, V. Q. Le, T.T. Nguyen, V.T. Nguyen, Sr doped LaMnO3 nanoparticles prepared by microwave combustion method: a recyclable visible light photocatalyst, Results Phys 19 (2020), 103417, https://doi.org/10.1016/j.rinp.2020.103417.

[5] T.H. Tran, T.C. Bach, N.H. Pham, Q.H. Nguyen, C.D. Sai, H.N. Nguyen, V. T. Nguyen, T.T. Nguyen, K.H. Ho, Q.K. Doan, Phase transition of $LaMnO_3$ nanoparticles prepared by microwave assisted combustion method, Mater. Sci. Semicond. Process. 89 (2019) 121–125, https://doi.org/10.1016/j.mssp.2018.09.002.

[6] T.H. Tran, V.T. Nguyen, Phase transition of Cu2O to CuO nanocrystals by selective laser heating, Mater. Sci. Semicond. Process. 46 (2016) 6–9, https://doi.org/10.1016/j.mssp.2016.01.021.

[7] Z. Liang, J. Zhou, L. Petti, L. Shao, T. Jiang, Y. Qing, S. Xie, G. Wu, P. Mormile, SERS-based cascade amplification bioassay protocol of miRNA-21 by using sandwich structure with biotin-streptavidin system, Analyst 144 (2019) 1741–1750, https://doi.org/10.1039/c8an02259c.

[8] M. Rippa, R. Castagna, D. Sagnelli, A. Vestri, G. Borriello, G. Fusco, J. Zhou, L. Petti, SERS biosensor based on engineered 2D-aperiodic nanostructure for in-situ detection of viable brucella bacterium in complex matrix, Nanomaterials 11 (2021) 7–9, https://doi.org/10.3390/nano11040886.

[9] M. Muniz-Miranda, C. Gellini, E. Giorgetti, Surface-enhanced Raman scattering from copper nanoparticles obtained by laser ablation, J. Phys. Chem. C 115 (2011) 5021–5027, https://doi.org/10.1021/jp1086027.

[10] A. Vincenzo, P. Roberto, F. Marco, M.M. Onofrio, I. Maria Antonia, Surface plasmon resonance in gold nanoparticles: a review, J. Phys. Condens. Matter 29 (2017), 203002. http://stacks.iop.org/0953-8984/29/i=20/a=203002.

[11] T.H.T. Nguyen, T.M.A. Nguyen, C.D. Sai, T.H.Y. Le, T.N. Anh Tran, T.C. Bach, V. V. Le, N.H. Pham, A.B. Ngac, V.T. Nguyen, T.H. Tran, Efficient surface enhanced Raman scattering substrates based on complex gold nanostructures formed by annealing sputtered gold thin films, Opt. Mater. (Amst). 121 (2021), 111488, https://doi.org/10.1016/j.optmat.2021.111488.

[12] N.A. Cinel, S. Cakmakyapan, S. Butun, G. Ertas, E. Ozbay, E-Beam lithography designed substrates for surface enhanced Raman spectroscopy, Photonics Nanostructures - Fundam. Appl. 15 (2015) 109–115, https://doi.org/10.1016/j.photonics.2014.11.003.

[13] L. Zhou, J. Zhou, W. Lai, X. Yang, J. Meng, L. Su, C. Gu, T. Jiang, E.Y.B. Pun, L. Shao, L. Petti, X.W. Sun, Z. Jia, Q. Li, J. Han, P. Mormile, Irreversible accumulated SERS behavior of the molecule-linked silver and silver-doped titanium dioxide hybrid system, Nat. Commun. 11 (2020) 1–10, https://doi.org/10.1038/s41467-020-15484-6.

[14] P. Sheng, W. Li, P. Du, K. Cao, Q. Cai, Multi-functional CuO nanowire/TiO2 nanotube arrays photoelectrode synthesis, characterization, photocatalysis and SERS applications, Talanta 160 (2016) 537–546, https://doi.org/10.1016/j.talanta.2016.07.043.

[15] X. Zhao, W. Zhang, C. Peng, Y. Liang, W. Wang, Sensitive surface-enhanced Raman scattering of TiO2/Ag nanowires induced by photogenerated charge transfer, J. Colloid Interface Sci. 507 (2017) 370–377, https://doi.org/10.1016/j.jcis.2017.08.023.

[16] A.E. Kandjani, M. Mohammadtaheri, A. Thakkar, S.K. Bhargava, V. Bansal, Zinc oxide/silver nanoarrays as reusable SERS substrates with controllable “hot-spots” for highly reproducible molecular sensing, J. Colloid Interface Sci. 436 (2014) 251–257, https://doi.org/10.1016/j.jcis.2014.09.017.

[17] Q.K. Doan, M.H. Nguyen, C.D. Sai, V.T. Pham, H.H. Mai, N.H. Pham, T.C. Bach, V. T. Nguyen, T.T. Nguyen, K.H. Ho, T.H. Tran, Enhanced optical properties of ZnO nanorods decorated with gold nanoparticles for self cleaning surface enhanced Raman applications, Appl. Surf. Sci. (2019), 144593, https://doi.org/10.1016/j.apsusc.2019.144593.

[18] J.P. Richters, T. Voss, D.S. Kim, R. Scholz, M. Zacharias, Enhanced surface-excitonic emission in ZnO/Al2O3 core-shell nanowires, Nanotechnology 19 (2008), https://doi.org/10.1088/0957-4484/19/30/305202.

[19] A.A. El-Bindary, S.M. El-Marsafy, A.A. El-Maddah, Enhancement of the photocatalytic activity of ZnO nanoparticles by silver doping for the degradation of AY99 contaminants, J. Mol. Struct. 1191 (2019) 76–84, https://doi.org/10.1016/j.molstruc.2019.04.064.

[20] T.H. Tran, T.H.T. Nguyen, M.H. Nguyen, N.H. Pham, A.B. Ngac, H.H. Mai, V. T. Pham, T.B. Nguyen, K.H. Ho, T.T. Nguyen, V.T. Nguyen, Synthesis of ZnO/Au nanorods for self cleaning applications, J. Nanosci. Nanotechnol. 21 (2021) 2621–2625, https://doi.org/10.1166/jnn.2021.19110.

[21] L. He, C. Ai, W. Wang, N. Gao, X. Yao, C. Tian, K. Zhang, An effective three-dimensional surface-enhanced Raman scattering substrate based on oblique Si nanowire arrays decorated with Ag nanoparticles, J. Mater. Sci. 51 (2016) 3854–3860, https://doi.org/10.1007/s10853-015-9704-7.

[22] H. Yang, Hybrid nanostructure of SiO2@Si with Au-nanoparticles for surface enhanced Raman spectroscopy. https://doi.org/10.1039/c9nr03813b, 2019, 13484,13493.

[23] P.M. Pancorbo, K. Thummavichai, L. Clark, T.A. Tabish, J. Mansfield, B. Gardner, H. Chang, N. Stone, Y. Zhu, Novel Au – SiO 2 – WO 3 core – shell composite nanoparticles for surface-enhanced Raman spectroscopy with potential application in cancer cell imaging, 1903549, https://doi.org/10.1002/adfm.201903549, 2019, 1,10.

[24] W. Rao, D. Wang, T. Kups, E. Baradács, B. Parditka, Z. Erdélyi, P. Schaaf, Nanoporous gold nanoparticles and Au/Al2O3 hybrid nanoparticles with large tunability of plasmonic properties, ACS Appl. Mater. Interfaces 9 (2017) 6273–6281, https://doi.org/10.1021/acsami.6b13602.

[25] T.H. Tran, M.H. Nguyen, T.H.T. Nguyen, V.P.T. Dao, Q.H. Nguyen, C.D. Sai, N. H. Pham, T.C. Bach, A.B. Ngac, T.T. Nguyen, K.H. Ho, H. Cheong, V.T. Nguyen, Facile fabrication of sensitive surface enhanced Raman scattering substrate based on CuO/Ag core/shell nanowires, Appl. Surf. Sci. 509 (2020), 145325, https://doi.org/10.1016/j.apsusc.2020.145325.

[26] T.H. Tran, M.H. Nguyen, T.H.T. Nguyen, V.P.T. Dao, P.M. Nguyen, V.T. Nguyen, N. H. Pham, V.V. Le, C.D. Sai, Q.H. Nguyen, T.T. Nguyen, K.H. Ho, Q.K. Doan, Effect of annealing temperature on morphology and structure of CuO nanowires grown by thermal oxidation method, J. Cryst. Growth 505 (2019) 33–37, https://doi.org/10.1016/j.jcrysgro.2018.10.010.

[27] L.N.H.F. Goldstein, Dai-sik Kim, Peter Y. Yu, L.C. Bournet, J.-P. Chaminade, Raman study of CuO single crystals, Phys. Rev. B 41 (1990) 7192–7194.

[28] T. Yu, X. Zhao, Z.X. Shen, Y.H. Wu, W.H. Su, Investigation of individual CuO nanorods by polarized micro-Raman scattering, J. Cryst. Growth 268 (2004) 590–595, https://doi.org/10.1016/j.jcrysgro.2004.04.097.

[29] S. Xie, D. Chen, C. Gu, T. Jiang, S. Zeng, Y.Y. Wang, Z. Ni, X. Shen, J. Zhou, Molybdenum oxide/tungsten oxide nano-heterojunction with improved surface-enhanced Raman scattering performance, ACS Appl. Mater. Interfaces 13 (2021) 33345–33353, https://doi.org/10.1021/acsami.1c03848.

[30] S. Hsieh, P.Y. Lin, L.Y. Chu, Improved performance of solution-phase surface-enhanced Raman scattering at Ag/CuO nanocomposite surfaces, J. Phys. Chem. C 118 (2014) 12500–12505, https://doi.org/10.1021/jp503202f.

[31] C. Zhu, G. Meng, P. Zheng, Q. Huang, Z. Li, X. Hu, X. Wang, Z. Huang, F. Li, N. Wu, A hierarchically ordered array of silver-nanorod Bundles for surface-enhanced Raman scattering detection of phenolic pollutants, Adv. Mater. 28 (2016) 4871–4876, https://doi.org/10.1002/adma.201506251.

[32] S. Yang, X. Dai, B.B. Stogin, T.S. Wong, Ultrasensitive surface-enhanced Raman scattering detection in common fluids, Proc. Natl. Acad. Sci. U. S. A. 113 (2016) 268–273, https://doi.org/10.1073/pnas.1518980113.

[33] P.J. Wass, D. Hollington, T.J. Sumner, Effective decrease of photoelectric emission threshold from gold plated surfaces Effective decrease of photoelectric emission threshold from gold plated surfaces. https://doi.org/10.1063/1.5088135, 2019.

[34] Q. Shi, G. Ping, X. Wang, H. Xu, J. Li, J. Cui, Photocatalyst for selective oxidation of methanol to methyl formate, J. Mater. Chem. A. 7 (2019) 2253–2260, https://doi.org/10.1039/c8ta09439j.

[35] M.E. Koleva, N.N. Nedyalkov, R. Nikov, R. Nikov, G. Atanasova, D. Karashanova, V.I. Nuzhdin, V.F. Valeev, A.M. Rogov, A.L. Stepanov, Fabrication of Ag/ZnO nanostructures for SERS applications, Appl. Surf. Sci. 508 (2020), 145227, https://doi.org/10.1016/j.apsusc.2019.145227.

[36] S. Sheng, Y. Ren, S. Yang, Q. Wang, P. Sheng, X. Zhang, Y. Liu, Remarkable SERS detection by hybrid Cu2O/Ag nanospheres, ACS Omega 5 (2020) 17703–17714, https://doi.org/10.1021/acsomega.0c02301.